

# RSC Advances



This is an *Accepted Manuscript*, which has been through the Royal Society of Chemistry peer review process and has been accepted for publication.

*Accepted Manuscripts* are published online shortly after acceptance, before technical editing, formatting and proof reading. Using this free service, authors can make their results available to the community, in citable form, before we publish the edited article. This *Accepted Manuscript* will be replaced by the edited, formatted and paginated article as soon as this is available.

You can find more information about *Accepted Manuscripts* in the [Information for Authors](#).

Please note that technical editing may introduce minor changes to the text and/or graphics, which may alter content. The journal's standard [Terms & Conditions](#) and the [Ethical guidelines](#) still apply. In no event shall the Royal Society of Chemistry be held responsible for any errors or omissions in this *Accepted Manuscript* or any consequences arising from the use of any information it contains.

# Luminescent properties of Milk Carbon Dots and their Sulphur and Nitrogen doped Analogues

Dan Wang, Xudong Wang, Yali Guo, Weisheng Liu, Wenwu Qin<sup>1</sup>

[Sep 25, 2014]

*Key Laboratory of Nonferrous Metal Chemistry and Resources Utilization of Gansu Province and State Key Laboratory of Applied Organic Chemistry, College of Chemistry and Chemical Engineering, Lanzhou University, Lanzhou 730000, P. R. China.*

---

<sup>1</sup> To whom correspondence should be addressed. E-mail for W. Qin: [qinww@lzu.edu.cn](mailto:qinww@lzu.edu.cn), Tel.: +86-931-8912582; Fax: +86-931-8912582

## Abstract

Carbon dots (CDs) and their L-cysteine (S doped CDs) and urea (N doped CDs) doped analogues were made by using the simple and low cost carbon source - pure milk. Milk-CDs have an average diameter of about  $5 \pm 0.27$  nm, whereas S doped CDs and N doped CDs have an average diameter of about  $4 \pm 0.07$  nm and  $3 \pm 0.07$  nm, respectively. The effect of the L-cysteine and urea doped on the spectroscopic and photophysical properties of Milk-CDs were studied by means of UV/vis absorption, steady-state, and time-resolved fluorometry. The maxima fluorescence excitation of S doped CDs and N doped CDs are blue-shifted by 40 and 60 nm and maxima fluorescence emission are blue shifted by 36 and 30 nm compared with those of the Milk-CDs, respectively. Furthermore, the maxima excitation of the up-conversion fluorescence emission (anti-Stokes) of N doped CDs are blue-shifted by 90 nm and emission maxima are blue shifted by 50 nm compared with those of the Milk-CDs and S doped CDs, respectively. N doped CDs have the highest fluorescence quantum yield among the three CDs. Moreover, the confocal microscopy experiments showed that Milk-CDs, S doped CDs and N doped CDs can be used within living cells.

## 1. Introduction

Carbon nanomaterials, such as carbon nanotubes,<sup>1</sup> fullerenes,<sup>2</sup> graphene<sup>3</sup> and nanofibers,<sup>4</sup> have been attracting much attention of researchers because of their valuable qualities. Recently, a new class of fluorescent carbon nanomaterials has emerged in the academic field - carbon dots (CDs), owing to their many advantages such as photostability, water solubility, biocompatibility, excellent cell membrane permeability and tuneable surface functionalities.<sup>5,6</sup> Compared to the traditional luminescent semiconductor quantum dots (QDs), which have been known for toxicity and potential environmental hazard due to the contained heavy metals,<sup>7,8</sup> the CDs are environmentally and biologically compatible.<sup>9</sup> As a result, much attention has been paid to their potential applications in biological labelling, bioimaging and drug delivery.<sup>10</sup>

It has been shown that precursors for CDs are simple and environmentally benign, and mainly include two types, chemical reagents and carbohydrates from daily life. For example, fluorescent carbon nanoparticles were prepared from the combustion soot of candles by means of an oxidative acid treatment,<sup>11</sup> which introduced OH and COOH groups to the carbon nanoparticles surfaces, thus, making the particles become negatively charged and hydrophilic. The other sources of CDs include carbohydrates from our daily life, such as soy milk,<sup>12</sup> sweet pepper,<sup>4</sup> paper ash<sup>13</sup> and banana juice,<sup>14</sup> whereas chemical reagents to synthesize CDs, could be for instance citric acid, L-cysteine, urea<sup>15-19</sup> and glycerol.<sup>7,20</sup>

Attention to the fluorescence up-conversion nanoparticles (UCNPs) has recently grown tremendously. They allow for transfer of a longer wavelength radiation (e.g. NIR light) to shorter wavelength fluorescence (e.g. visible light) via a two-photon or multiphoton mechanism.<sup>21</sup> When it comes to the synthetic aspect of the up-conversion nanoparticles, a lot of methodologies to

synthesize UCNPs with desirable properties have been reported. However, to date most of the up-conversion fluorescent materials reported are inorganic crystals doped with rare-earth elements, such as NaYF<sub>4</sub>: Yb<sup>3+</sup>, Er<sup>3+</sup><sup>22</sup> and NaGdF<sub>4</sub>: Yb/Er.<sup>23</sup> To the best of our knowledge, there are only a few nanomaterials displaying both down and up-conversion fluorescence, but interestingly it has been shown that carbon dots have the down and up-conversion fluorescence properties.<sup>24,25</sup> Therefore, CDs prepared from green materials with excellent up-conversion fluorescent properties have aroused the interest of researchers.

In the present paper, carbon dots (Milk-CDs) and their L-cysteine (S doped CDs) and urea (N doped CDs) doped analogues were made by using the simple and accessible carbon source - pure milk, by a one-step hydro-thermal reaction. The method has many advantages such as cheap raw materials, environmental compatibility and mild reaction conditions. The spectroscopic properties and the photophysical characteristics of Milk-CDs, S doped CDs and N doped CDs analogues derivative were investigated by using UV/vis absorption, and steady-state and time-resolved fluorescence spectroscopy. The effect of the L-cysteine and urea on the spectroscopic and photophysical properties of CDs is reported. The photophysical characteristics of the studied CDs analogs strongly depend on the nature of the materials doped with heteroatoms.

## 2. Experimental

### 2.1 Chemicals

Pure milk was purchased from the local supermarket and was not treated. Urea (>99.0%) and L-cysteine (99%) were purchased from Guangfu (Tianjin) and J&K (Beijing). All solvents and reagents were of analytical grade and directly used without any further purification.

### 2.2 Instrument

XRD measurements were performed on a X-ray diffract meter (D/max-2400pc, Rigaku, Japan) with Cu K $\alpha$  radiation ( $\lambda = 1.54178 \text{ \AA}$ ), with the operation voltage and current at 40 kV and 60 mA, respectively. The  $2\theta$  range was from 10 to 50° in steps of 0.02°. The transmission electron microscopy (TEM) was obtained on a JEM-2100 transmission electron microscope at an acceleration voltage of 120 kV. Samples were prepared by placing a drop of a dilute alcohol dispersion of the products on the surface of a copper grid. Dynamic light scattered (DLS) was got on a BI-200SM (USA Brookhaven) at room temperature. Elemental was obtained by a Vario cude (Germany). The atomic force microscopy (AFM) images were obtained using a tapping mode of Agilent 7000 Atomic Force Microscope. Raman spectra were measured with a Renishaw InVia Raman microscope at room temperature with a 633 nm line laser as the excitation source. Fourier transform infrared (FTIR) spectra were conducted within the 4000-400  $\text{cm}^{-1}$  wavenumber range using a Nicolet 360 FTIR spectrometer with the KBr pellet technique.

### **2.3 Steady-state UV–vis absorption and fluorescence spectroscopy**

UV–vis absorption spectra were recorded on a Varian UV-Cary100 spectrophotometer, and for the corrected steady-state excitation and emission spectra and up-conversion fluorescence spectra, a FLS920 spectrofluorometer was employed. Freshly prepared samples in 1 cm quartz cells were used to perform all UV–vis absorption and emission measurements.

Quantum yields were determined by an absolute method using an integrating sphere based upon that originally developed by de Mello<sup>26</sup> et al. Experiments were conducted on an FLS920 from Edinburgh Instruments.

### **2.4 Time-Resolved Fluorescence Spectroscopy**

Fluorescence decay times were measured on an Edinburgh Instruments FLS920 equipped with the light emitting diodes (excitation wavelengths 330, 360 and 375 nm), using the time-correlated single photon counting technique<sup>27,28</sup> in 2048 channels at room temperature. The samples were dissolved in water and the concentrations were adjusted to have optical densities at the excitation wavelength (330, 360 and 375 nm) < 0.1. The monitored wavelengths were 420nm, 440 nm, and 460 nm.

Histograms of the instrument response functions (using a LUDOX scatter) and sample decays were recorded until they typically reached  $1.0 \times 10^4$  counts in the peak channel. Obtained histograms were fitted as sums of the exponentials, using Gaussian-weighted nonlinear least squares fitting based on Marquardt-Levenberg minimization implemented in the software package of the instrument. The fitting parameters (decay times and preexponential factors) were determined by minimizing the reduced chi-square  $\chi^2$ . An additional graphical method was used to judge the quality of the fit that included plots of surfaces (“carpets”) of the weighted residuals vs channel number. All curve fittings presented here had  $\chi^2$  values < 1.1.

## 2.5 Cell Culture

The SMMC-7721 cells were provided by the Institute of Biology (Lanzhou University). To determine the cell permeability of CDs and their analogues, the cells were incubated with 50  $\mu\text{M}$  of CDs and their analogues (water) for 1h at 37 °C, and washed with 4-(2-Hydroxyethyl)-1-piperazineethanesulfonic acid (HEPES) to remove the remaining CDs. The confocal fluorescence image was observed using a confocal microscope - Leica DM-4000D microscope (excited by blue and ultraviolet light).

## 2.6 Synthesis of Milk-CDs

The Milk-CDs were prepared by hydro-thermal treatment with the single carbon source - pure milk. Then, it was transferred into a 25 mL Teflon-lined autoclave and heated at 180 °C for 8 h. In order to check the effect of preparation time on the fluorescence properties, Milk-CDs were heated over different time (2, 3, 5 and 8 hours).

The CDs were collected by removing the large nanoparticles by centrifugation at 8000 rpm for 20 min and pouring out the unreacted precursors. Finally, the obtained Milk-CDs were dispersed in ultrapure water.

### **2.7 Synthesis of S doped CDs**

2g of pure milk and 1g of L- cysteine were transferred into a 25 mL Teflon-lined autoclave and heated at 180 °C for 8 h. The CDs were obtained by removing the large nanoparticles by centrifugation at 8000 rpm for 20 min and pouring out the unreacted precursors. Finally, the obtained S doped CDs were dispersed in ultrapure water.

### **2.8 Synthesis of N doped CDs**

10g of pure milk and 5g of urea were transferred into a 25 mL Teflon-lined autoclave and heated at 180 °C for 8 h. The CDs were collected by removing the large nanoparticles by centrifugation at 8000 rpm for 20 min and pouring out the unreacted precursors. Finally, the obtained N doped CDs were dispersed in ultrapure water.

## **3. Results and discussions**

We have chosen a variety of carbon precursor materials to prepare the carbon dots, such as citric acid, carrots and pure milk. However, considering the fluorescence properties and inexpensive green raw resource, in the present report we selected the pure milk as carbon



precursor material to synthesize the CDs.

The effect of heating time on the fluorescence quantum yield of prepared CDs using carrots and pure milk is shown in the Table S1 (Supporting Information). The results show that the fluorescence quantum yield of prepared CDs reaches a stable value after 8 hours (Figure 1). The maxima in the emission spectra are also affected by the heating time; the maximum being slightly shifted hypsochromically on prolonging preparation from 2h [ $\lambda_{em(max)}=486$  nm] to 8h [ $\lambda_{em(max)}=466$  nm]. Therefore, the final investigated CDs and their analogues were all prepared during 8 hours.

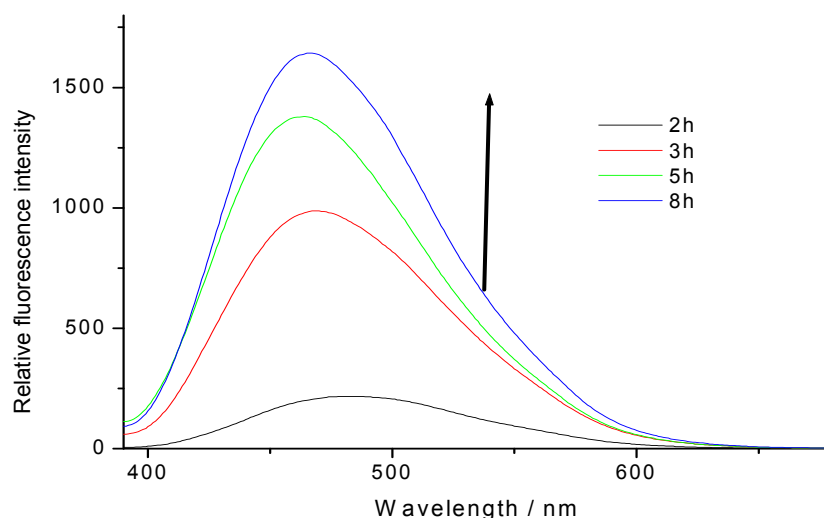


**Figure 1** The effect of the preparation time (2, 3, 5, 8h) of Milk-CDs on the fluorescence emission intensity ( $\lambda_{ex} = 360$ nm).

The Milk-CDs, S doped CDs and N doped CDs were synthesized and characterized by TEM, DLS, AFM, XRD, FT-IR, Raman and elemental analysis. Like most reported CDs, the prepared Milk-CDs, S doped CDs, N doped CDs all show bright blue luminescence under excitation of 365 nm UV-lamp.

Elemental analyses indicate that the CDs are mainly composed of carbon, nitrogen, oxygen and sulphur, as shown in Table S2. The contents of S and N in the prepared S doped CDs and N doped CDs, respectively, have been improved.

As revealed by transmission electron microscopy (TEM) and dynamic light scattered (DLS), figure 2 demonstrates the morphology and size of the prepared Milk-CDs, S doped CDs and N doped CDs. The morphology of prepared Milk-CDs (Figure 2a) is regularly spherical with an average diameter about  $5 \pm 0.27$  nm, whereas S doped CDs and N doped CDs have an average diameter of about  $4 \pm 0.07$  nm and  $3 \pm 0.07$  nm (Figure 2b and 2c), respectively. Dynamic light scattering (DLS) analysis at room temperature also shows that the average hydrodynamic diameter of Milk-CDs, S doped CDs and N doped CDs is  $5 \pm 0.27$  nm,  $4 \pm 0.07$  nm and  $3 \pm 0.07$  nm (Figure 2), respectively. The atomic force microscopy (AFM) image (Figure S1) shows the topographic height and surface roughness of the obtained CDs. The Milk-CDs (Figure S1a) shows the topographic height mostly distributed in the range from 0 to 5.59 nm, with an average value of about 2.80 nm. And the average value of the S doped CDs (Figure S1b) and N doped CDs (Figure S1c) is respectively about 2.34 and 1.91 nm. The surface roughness of the obtained CDs is 0.954, 1.01 and 0.685, which should be as small as possible.

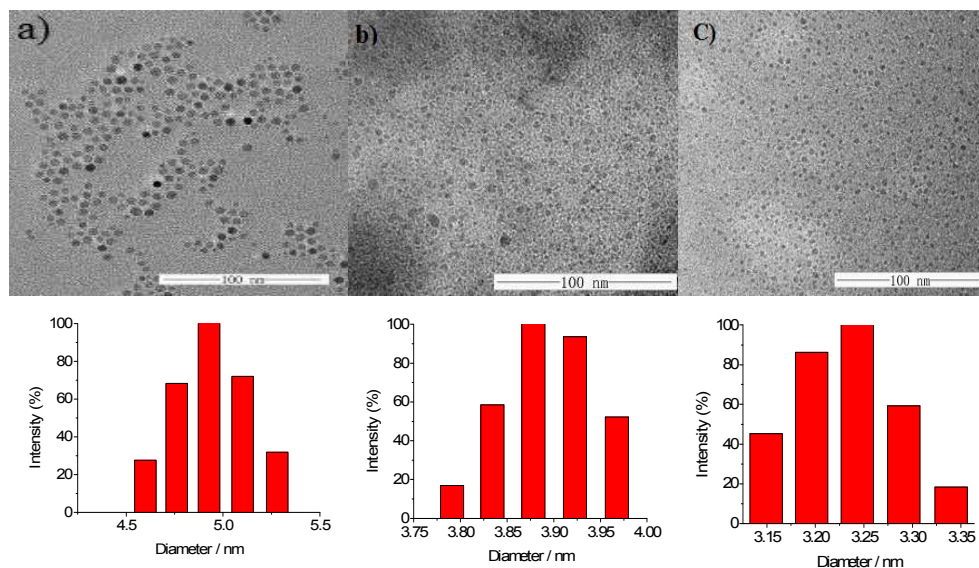


**Figure 2** TEM of Milk-CDs (a); S doped CDs (b); N doped CDs (c); below figures are the particle size distribution of the prepared CDs (nm) respectively.

The X-ray diffraction (XRD) pattern is presented in figure S2. The typical XRD profiles of CDs consist of wider diffraction peaks centered at around  $22.0^\circ$  which have an interlayer spacing of about 0.396 nm and is bigger than that of graphite (0.34 nm).<sup>4</sup>

IR spectra of Milk-CDs, S doped CDs and N doped CDs are shown in figure S3 and S4a. We characterized the CDs obtained by different preparation time and found that they were similar. In the IR spectra of Milk-CDs, the vibration band at about  $3367.1\text{ cm}^{-1}$  is attributed to OH group. The vibration band at about  $2853\text{ cm}^{-1}$  and  $1746\text{ cm}^{-1}$  indicates the presence of the carbonyl group in the surface of prepared CDs. In the IR spectra of S doped CDs, the vibration bands at about  $1636\text{ cm}^{-1}$ ,  $1401\text{ cm}^{-1}$  and  $1048\text{ cm}^{-1}$  clearly indicate the existence of S=C, C-N and C-S groups. In the IR spectra of N doped CDs, the vibration band at about  $3370\text{ cm}^{-1}$  is attributed to  $\delta\text{OH}$  and  $\delta\text{NH}$  vibrations. The vibration band at about  $2921\text{ cm}^{-1}$  and  $1672\text{ cm}^{-1}$  indicates the presence of the carbonyl group in the surface of prepared CDs. And the vibration

of about  $1404\text{ cm}^{-1}$  is attributed to the C-N.

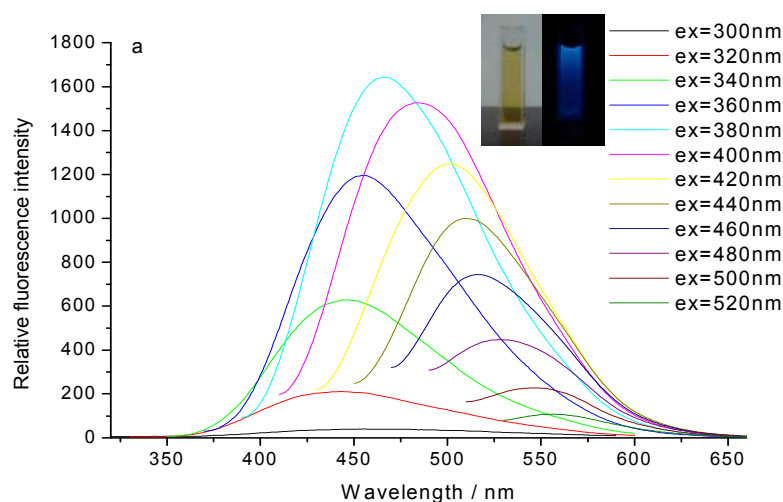
The carbon structures of Milk-CDs and their analogues were confirmed by their respective Raman spectra excited at 633 nm (Fig. S4b). The broad peak at  $1347\text{ cm}^{-1}$  is assigned to the D band, which corresponds to the  $\text{sp}^3$  defects in CDs. The peak at  $1629\text{ cm}^{-1}$  matches well with the G band, which is a band related to the in-plane bond-stretching motion of C  $\text{sp}^2$  atoms, indicating that there are olefinic groups inside C-dots.

UV/Vis absorption spectra of Milk-CDs dissolved in water are depicted in figure S5. The absorption spectra are of similar shape as those of described CDs.<sup>29,30</sup> Milk-CDs show broad absorption bands with absorption maxima at 275 nm attributed to  $\pi\text{-}\pi^*$  transition of the C=C band. The absorption spectrum of S doped CDs exhibits two bands wherein one in the region of 274 nm and another at around 310 nm are attributed to  $\pi\text{-}\pi^*$  transition of the C=C band and  $\text{n-}\pi^*$  transition of the C=S band, respectively. On closer inspection in Figure S5, however, the N doped CDs shows the two absorption peaks at around 274nm and 310nm, which is not very clear compared to the S doped CDs.<sup>31</sup> We consider that the additional peak of the S doped CDs and N doped CDs maybe due to the introduced heteroatoms S and N with the lone electron pairs.

It has been reported that the fluorescence emission spectra and photoluminescent intensity of CDs depend on the excitation wavelength.<sup>32, 33</sup> The prepared carbon dots exhibited a bright blue-green colour under ultraviolet radiation ( $\lambda_{\text{ex}} = 365\text{ nm}$ ). The optical photos of the three CDs recorded at room light and UV-lamp irradiation are shown in Figure 3 and Figure S6. In figure 3a, the maximum of the fluorescence emission ( $\sim 466\text{ nm}$ ) of Milk-CDs (8h) was obtained with an excitation wavelength of 380 nm, whereas increased excitation wavelength shifted the emission, which may be attributed to the optical selection of differently-sized nanoparticles (quantum

effect) and a distribution of the different surface energy traps of the carbon dots. The fluorescent emission intensity for Milk-CDs decreases with the increased excitation wavelength (longer than 380 nm).

Figure 3b displays the fluorescence emission spectra of Milk-CDs, S doped CDs and N doped CDs at different excitation wavelength (360 and 420nm). It is clear that the photoluminescent intensity of the N doped CDs is the strongest, is in accordance with the fluorescence quantum yield (FLQY) shown in Table S3. The QY increases with the excitation wavelength and the value reaches the peak at 360 nm, and decreases at 380nm. At the excitation wavelength of 360nm the FLQY of the N doped CDs of has been improved 1.59 times compared to the Milk-CDs.



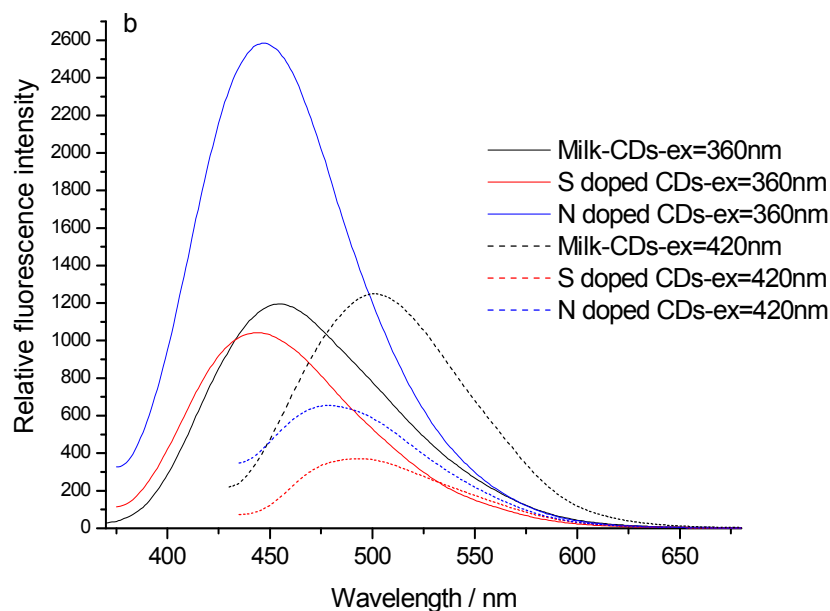


**Figure 3** Fluorescence emission spectra of (a) Milk-CDs (8h); (b) Milk-CDs, S doped CDs and N doped CDs dispersed in water excited at different excitation wavelengths. The inset shows the photos of the cuvettes containing Milk-CDs recorded at room light and under UV-lamp irradiation.

Introduction of L- cysteine (S doped CDs) and urea (N doped CDs) causes large blue shifts in both the excitation and emission spectra of the investigated CDs analogues. For example, the fluorescence excitation and emission maxima [ $\lambda_{\text{ex}}(\text{max})$  and  $\lambda_{\text{em}}(\text{max})$ , respectively] of S doped CDs [ $\lambda_{\text{ex}}(\text{max})=340$  nm and  $\lambda_{\text{em}}(\text{max})=430$  nm] are blue-shifted by  $\sim 40$  nm and  $\sim 36$  nm compared to Milk-CDs [ $\lambda_{\text{ex}}(\text{max})=380$  nm and  $\lambda_{\text{em}}(\text{max})=466$  nm], whereas  $\lambda_{\text{ex}}(\text{max})$  and  $\lambda_{\text{em}}(\text{max})$  of N doped CDs [ $\lambda_{\text{ex}}(\text{max})=320$  nm and  $\lambda_{\text{em}}(\text{max})=435$  nm] are blue-shifted by  $\sim 60$  nm and  $\sim 30$  nm compared to the corresponding Milk-CDs (Figure 3b and Figure S6-S7).

The very strong up-conversion fluorescence can also be measured with the strong emission fluorescence in the 400 - 600 nm range upon excitation wavelengths from 600 to 880 nm (Figure 4 and Figure S8). This excitation dependent feature and anti-Stokes type emission may

be attributed to the distribution of different particle sizes of the CDs, different emissive sites on each CD and the multiphoton active processes.<sup>4</sup> The excitation and emission maxima [ $\lambda_{\text{ex}}(\text{max})$  and  $\lambda_{\text{em}}(\text{max})$ ] of up-conversion fluorescence emission spectra of N doped CDs [ $\lambda_{\text{ex}}(\text{max})=760$  nm and  $\lambda_{\text{em}}(\text{max})=456$  nm] are blue-shifted by  $\sim 90$  nm and  $\sim 50$  nm compared to Milk-CDs and S doped CDs [ $\lambda_{\text{ex}}(\text{max})=850$  nm and  $\lambda_{\text{em}}(\text{max})=506$  nm] (Figure 4a and Figure S7). Figure 4b displays the up-conversion fluorescence emission spectra of Milk-CDs, S doped CDs and N doped CDs at different excitation wavelength (760 and 850nm).

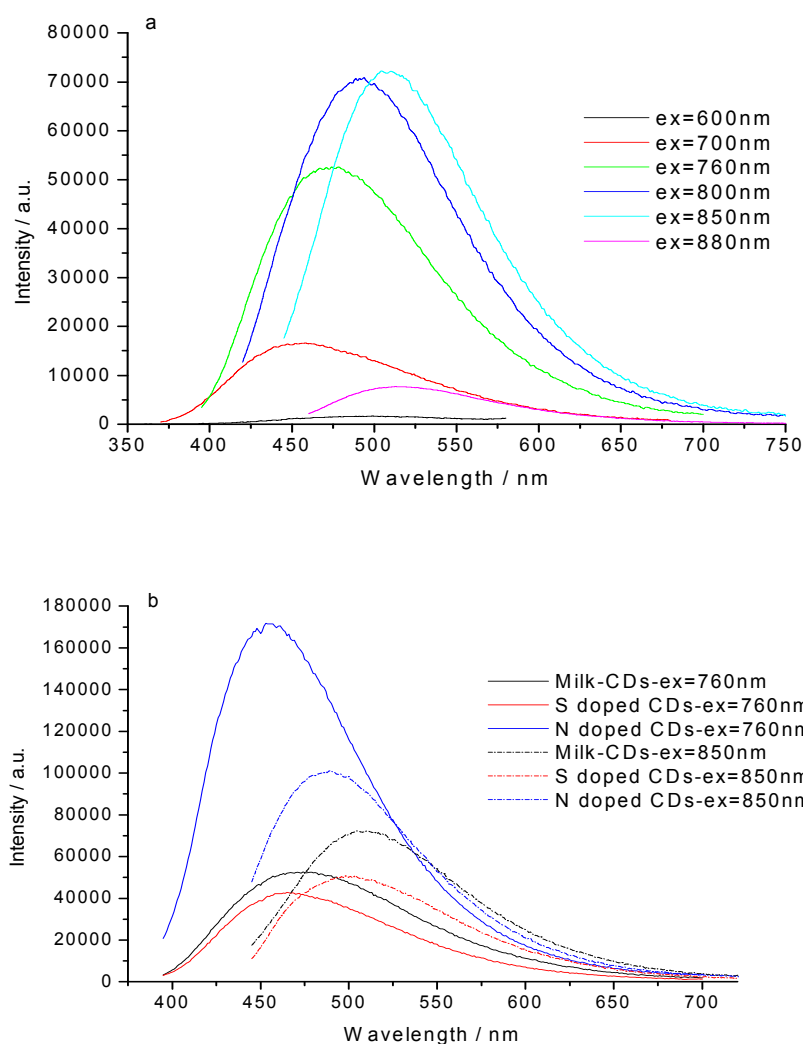


**Figure 4** Up-conversion fluorescence emission spectra of the (a) Milk-CDs and (b) Milk-CDs, S

doped CDs and N doped CDs dispersed in water excited at different excitation wavelengths.

To investigate the fluorescence dynamics of CDs and their analogues, fluorescence decay traces of CDs and their analogues in water were collected as a function of emission wavelength  $\lambda_{em}$  by the single-photon timing technique. Each fluorescence decay trace was analyzed individually as a sum of three exponential functions in terms of decay times  $\tau_i$  and the associated pre-exponential factors  $\alpha_i$  ( $i = 1 - 3$ ). Mono- or bi-exponential decay functions failed to describe the observed decays as evidenced by the large  $\chi^2$  and high non-random residuals. Table S4 – S6 summarize the time resolved fluorescence data and the average lifetimes<sup>34, 35</sup> of CDs and their analogues in water.

Before an attempt is made to analyze the results, it is worth recapitulating the literature data on CDs. For CDs in ethanol, a tri-exponential function ( $\sim 1.0$  ns,  $\sim 5.0$  ns and  $\sim 13.0$  ns) was used to fit the decay at all three emission wavelengths.<sup>6</sup> The fluorescence decay of Milk-CDs in water at  $\lambda_{ex} = 360$  nm also displays tri-exponential behavior, and a tri-exponential function ( $\sim 0.8$  ns,  $\sim 3.5$  ns and  $\sim 11.0$  ns) was used to fit the decays at all three emission wavelengths. The fast component ( $\tau_1 \sim 0.8$  ns) has the amplitude of about  $\sim 20$  %, whereas the contributions of the  $\tau_2$  ( $\sim 3.5$  ns) and  $\tau_3$  ( $\sim 11.0$  ns) components are about  $\sim 47$  % and  $\sim 33$  %, respectively. The decay times are similar to those reported in the literature.<sup>6, 18, 36</sup> The different preparation time of Milk-CDs does not induce a clear change of the fluorescence decays.

The decay times of S doped CDs in water are similar to those of Milk-CDs in water. For S doped CDs in water, a tri-exponential function ( $\sim 0.7$  ns,  $\sim 3.5$  ns and  $\sim 11.0$  ns) was used to fit the decay at all three emission wavelengths. On the other hand, the fluorescence decay of N doped CDs is different from that of Milk-CDs and S doped CDs. The fast component (decay time  $\tau_1 \approx 1.3$  ns) became slower (Figure 5). Whereas the results of fluorescence decay of  $\tau_2$  and  $\tau_3$  of N



doped CDs are similar to those of Milk-CDs and S doped CDs. It can be seen from table S4-S5 that the third lifetime  $\tau_3$  (or sum of  $\tau_2 + \tau_3$ ) of Milk-CDs has a largest contribution. We also measured the decay times of the CDs and their analogues, excited at 330 and 375 nm giving somewhat different results (shown in Table S4 – S6).

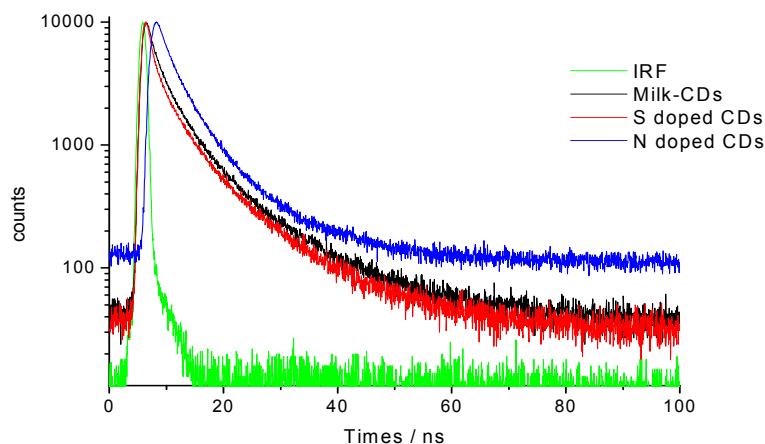
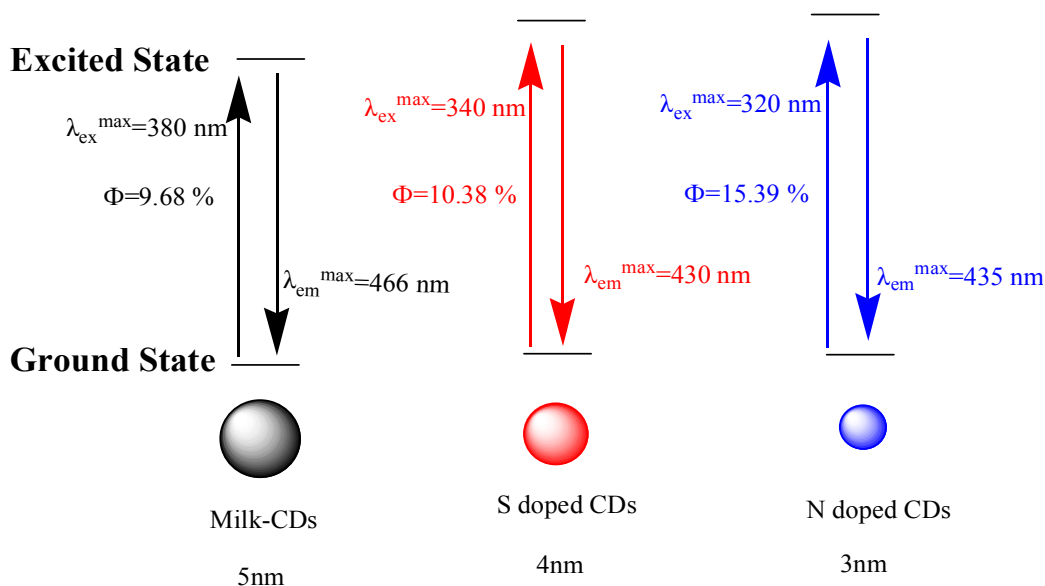


**Figure 5** The decay curves of Milk-CDs, S doped CDs and N doped CDs in water collected at 440nm when excited at 360 nm.

The fluorescence decays of CDs and their analogues in water are complicated, probably due to the involvement of different particle sizes and the distribution of the different surface energy traps of CDs in solution. In water, most likely three different particle sizes are present. The difference of fluorescence properties is due to the variation in size of the carbon dots. The energy gap increases with the decrease in size of the carbon dots. Further investigations are necessary and will be undertaken. N doped CDs have the smallest particle size (~3 nm) among the CDs studied. The maxima in the excitation spectra of N doped CDs are blue-shifted by 60 nm and fluorescence maxima are blue shifted by 30 nm compared to those of the CDs. Furthermore, the excitation of the up-conversion fluorescence emission (anti-Stokes) of N doped CDs is

blue-shifted by 90 nm and fluorescence maximum is blue shifted by 50 nm compared to those of the Milk-CDs and S doped CDs. N doped CD has the highest fluorescence quantum yield and longer lifetime. The photophysical results are in accordance with the steady state measurements (Scheme 1).



**Scheme 1** Simplified photophysical properties scheme of Milk-CDs, S doped CDs and N doped CDs.

#### 4. Fluorescence images

For practical applications, it is necessary to detect the molecular probe is in living cells under biological conditions using a confocal microscope. SMMC-7721 cells (Human liver cancer cells) were incubated with Milk-CDs, S doped CDs and N doped CDs (50  $\mu\text{M}$ , water). After incubation for 1 hour at 37  $^{\circ}\text{C}$  SMMC-7721 cells display different fluorescence when excited at different wavelengths (ultraviolet light and blue light), as shown in figure 6. Figure 6a shows the bright field microscopy image of the cells. The cells incubated with Milk-CDs show blue fluorescence when excited by ultraviolet light (Figure 6-2b), whereas the cells incubated with S doped CDs and N

doped CDs show brighter blue fluorescence (Figure 6-3b and Figure 6-4b). The finding may be due to the easier internalization of the S doped CDs and N doped CDs into the cells compared to Milk-CDs. As we mentioned before, with increasing excitation wavelength, the intensity of the emission band of CDs decreases, while the maximum of the band shifts to the red. When changing the excitation wavelength from ultraviolet light to blue light, the cells incubated with S doped CDs display the brightest green fluorescence (Figure 6-3c). The finding is in accordance with the fluorescence emission of the S doped CDs shown in the figure S5, the S doped CDs shows the highest fluorescence intensity at the long wavelength (~460 nm) compared to Milk-CDs and N doped CDs.

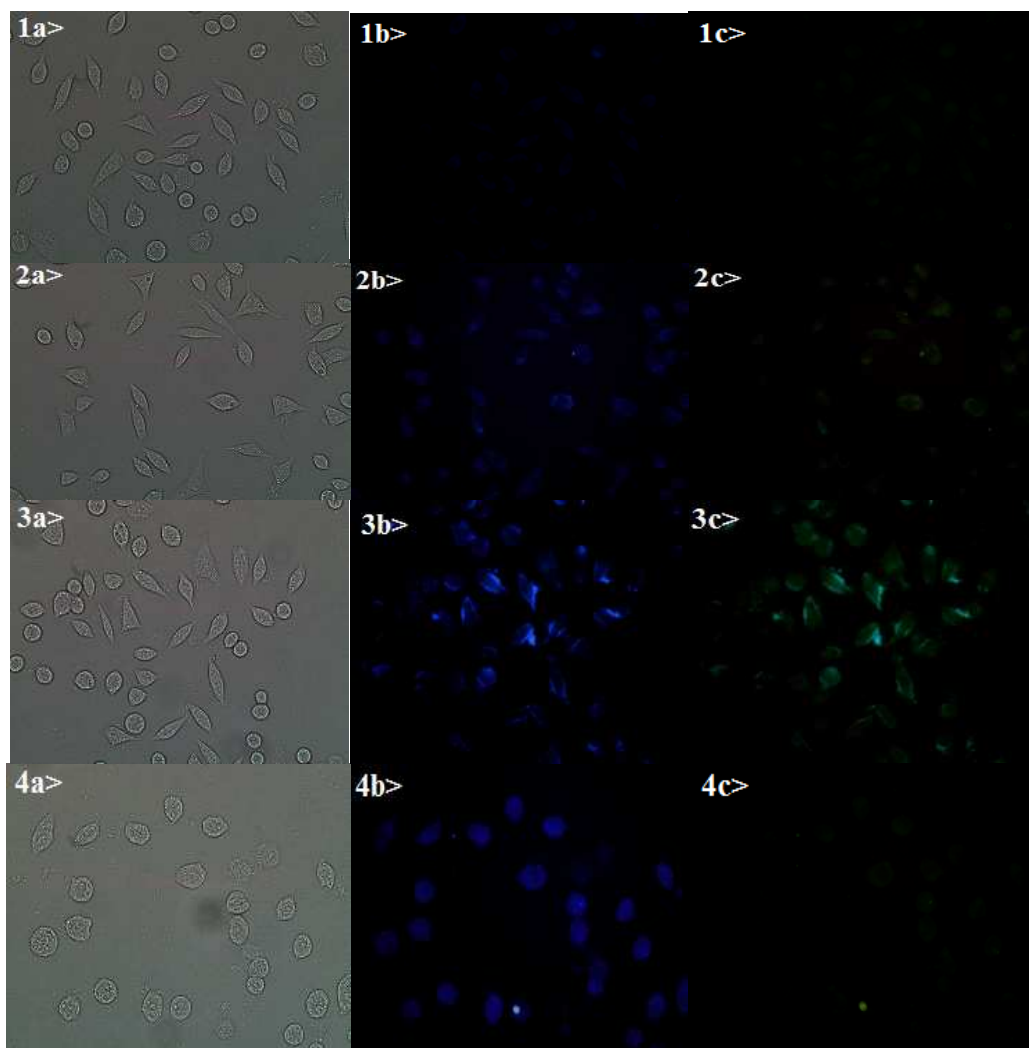


**Figure 6** Confocal fluorescence images of live SMMC-7721 cells. The excited light is ultraviolet (b) and blue light (c). (1) 1a-Bright field microscopy image of pure SMMC-7721 cells, 1b- Fluorescence image of pure SMMC-7721 cells excited by ultraviolet light and 1c- Fluorescence image of pure SMMC-7721 cells excited by blue light (2) Fluorescence image of SMMC-7721 cells incubated with 50  $\mu\text{M}$  Milk-CDs (water) for 1 hour at 37  $^{\circ}\text{C}$ . (3) Fluorescence image of SMMC-7721 cells incubated with 50  $\mu\text{M}$  S doped CDs (water) for 1 hour at 37  $^{\circ}\text{C}$ . (4) Fluorescence image of SMMC-7721 cells incubated with 50  $\mu\text{M}$  N doped CDs (water) for 1 hour at 37  $^{\circ}\text{C}$ .

## 5. Conclusion

In summary, carbon dots (CDs) and their L-cysteine (S doped CDs) and urea (N doped CDs) doped analogues were made by using the simple and accessible carbon source - pure milk. Milk-CDs have an average diameter of about  $5 \pm 0.27$  nm, whereas S doped CDs and N doped CDs have an average diameter of about  $4 \pm 0.07$  nm and  $3 \pm 0.07$  nm, respectively. Due to the involvement of different particle sizes and the distribution of the different surface energy traps of CDs, the photophysical properties of Milk-CDs, S doped CDs and N doped CDs in water are quite different. The maxima in the fluorescence excitation and emission spectra and up-conversion fluorescence emission (anti-Stokes) spectra of the S doped CDs and N doped CDs exhibit the clear blue-shift compared to the Milk-CDs. N doped CDs have the highest fluorescence quantum yield among the CDs studied. They offer, not only the down conversion fluorescence properties, but also the strong up-conversion fluorescence. Moreover, confocal microscopy experiments showed that CDs can be used within living cells. Such multifunctional nanoparticles should have great potentials for wider application.

### **Acknowledgement**

This work was supported by the National Science Foundation for Fostering Talents in Basic Research of the National Natural Science Foundation of China (Grant No. J1103307) and the “International Cooperation Program of Gansu Province” (1104WCGA182). The authors would like to thank the Natural Science Foundation of China (No. 21271094), and this study was supported in part by the “Key Program of National Natural Science Foundation of China” (20931003).

## Notes and references

Key Laboratory of Nonferrous Metal Chemistry and Resources Utilization of Gansu Province and State Key Laboratory of Applied Organic Chemistry, College of Chemistry and Chemical Engineering, Lanzhou University, Lanzhou 730000, P. R. China. [qinww@lzu.edu.cn](mailto:qinww@lzu.edu.cn)

- [1] B. L. Liu, C. Wang, J. Liu, Y. C. Che, C. W. Zhou, *Nanoscale*, 2013, **5**, 9483-9502.
- [2] J. B. Hooper, D. Bedrov, G. D. Smith, *Phys. Chem. Chem. Phys.*, 2009, **11**, 2034-2045.
- [3] X. Huang, J. Chen, H. Yu, R. Cai, S. J. Peng, Q. Y. Yan, H. H. Hng, *J. Mater. Chem. A*, 2013, **1**, 6901-6907.
- [4] B. D. Yin, J. H. Deng, X. Peng, Q. Long, J. N. Zhao, Q. J. Lu, Q. Chen, H. T. Li, H. Tang, Y. Y. Zhang, S. Z. Yao, *Analyst*, 2013, **138**, 6551-6557.
- [5] (a) O. Kozák, K. K. R. Datta, M. Greplová, V. Ranc, J. K. lík, R. Zbořil, *J. Phys. Chem. C*, 2013, **117**, 24991-24996.
- (b) C. M. Yu, X. Z. Li, F. Zeng, F. Y. Zheng, S. Z. Wu, *Chem. Commun.*, 2013, **49**, 403-405.
- [6] D. Wang, Y. L. Guo, W. S. Liu, W. W. Qin, *RSC Adv.*, 2014, **4**, 7435-7439.
- [7] (a) X. H. Wang, K. G. Qu, B. L. Xu, J. S. Ren, X. G. Qu, *J. Mater. Chem.*, 2011, **21**, 2445-2450.
- (b) Y. P. Sun, X. Wang, F. S. Lu, L. Cao, M. J. Mezziani, P. G. Luo, L. R. Gu, L. M. Veca, *J. Phys. Chem. C*, 2008, **112**, 18295-18298.
- (c) S. Roy, C. Tuinenga, F. Fungura, P. Dagtepe, V. Chikan, *J. Phys. Chem. C*, 2009, **113**, 13008-13015.
- (d) S. T. Yang, X. Wang, H. F. Wang, F. S. Lu, P. J. G. Luo, L. Cao, M. J. Mezziani, J. H. Liu, Y. F. Liu, M. Chen, Y. P. Huang, Y. P. Sun, *J. Phys. Chem. C*, 2009, **113**, 18110-18114.
- [8] D. Chowdhury, N. Gogoi, G. Majumdar, *RSC Adv.*, 2012, **2**, 12156-12159.
- [9] L. L. Li, G. H. Wu, G. H. Yang, J. Peng, J. W. Zhao, J. J. Zhu, *Nanoscale*, 2013, **5**, 4015-4039.
- [10] C. W. Lai, Y. H. Hsiao, Y. K. Peng, P. T. Chou, *J. Mater. Chem.*, 2012, **22**, 14403-14409.
- [11] H. P. Liu, T. Ye, C. D. Mao, *Angew. Chem. Int. Ed.*, 2007, **46**, 6473-6475.
- [12] C. Z. Zhu, J. F. Zhai, S. J. Dong, *Chem. Commun.*, 2012, **48**, 9367-9369.
- [13] J. M. Wei, J. M. Shen, X. Zhang, S. K. Guo, J. Q. Pan, X. G. Hou, H. B. Zhang, L. Wang, B. X. Feng, *RSC Adv.*, 2013, **3**, 13119-13122.
- [14] B. De, N. Karak, *RSC Adv.*, **2013**, **3**, 8286-8290.
- [15] Y. Q. Dong, H. C. Pang, H. B. Yang, C. X. Guo, J. W. Shao, Y. W. Chi, C. M. Li, T. Yu, *Angew. Chem. Int. Ed.*, 2013, **52**, 7800-7804.

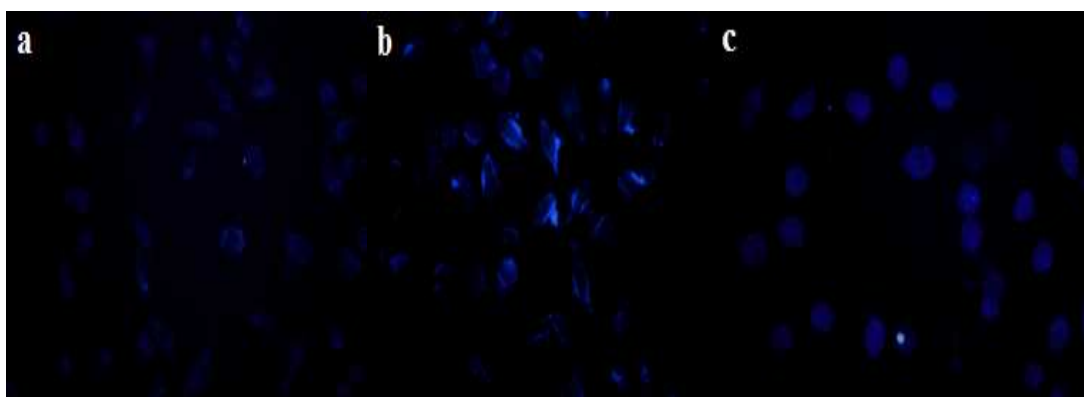
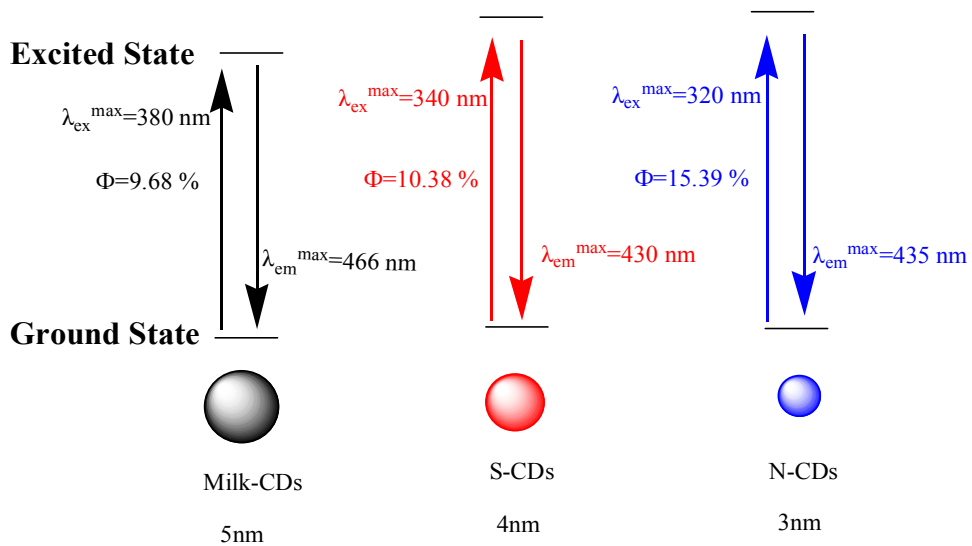
- [16] Y. Q. Dong, R. X. Wang, H. Li, J. W. Shao, Y. W. Chi, X. M. Lin, G. N. Chen, *Carbon*, 2012, **50**, 2810-2815.
- [17] Y. Q. Dong, J. W. Shao, C. Q. Chen, H. Li, R. X. Wang, Y. W. Chi, X. M. Lin, G. N. Chen, *Carbon*, 2012, **50**, 4738-4743.
- [18] S. Chandra, P. Patra, S. H. Pathan, S. Roy, S. Mitra, A. Layek, R. Bhar, P. Pramanik, A. Goswami, *J. Mater. Chem. B*, 2013, **1**, 2375-2382.
- [19] J. Zhou, Y. Yang, C. Y. Zhang, *Chem. Commun.*, 2013, **49**, 8605-8607.
- [20] C. J. Liu, P. Zhang, F. Tian, W. C. Li, F. Li, W. G. Liu, *J. Mater. Chem.*, 2011, **21**, 13163-13167.
- [21] L. Zhou, Z. H. Li, Z. Liu, M. L. Yin, J. S. Ren, X. G. Qu, *Nanoscale*, 2014, **6**, 1445-1452.
- [22] C. N. Zhong, P. P. Yang, X. B. Li, C. X. Li, D. Wang, S. L. Gai, J. Lin, *RSC Adv.*, 2012, **2**, 3194-3197.
- [23] C. X. Li, Z. Y. Hou, Y. L. Dai, D. M. Yang, Z. Y. Cheng, P. A. Ma, J. Lin, *Biomater. Sci.*, 2013, **1**, 213-223.
- [24] H. T. Li, X. D. He, Y. Liu, H. Huang, S. Y. Lian, S. T. Lee, Z. H. Kang, *Carbon*, 2011, **49**, 605-609.
- [25] S. J. Zhu, J. H. Zhang, X. Liu, B. Li, X. F. Wang, S. J. Tang, Q. N. Meng, Y. F. Li, C. Shi, R. Hu, B. Yang, *RSC Adv.*, 2012, **2**, 2717-2720.
- [26] J. C. de Mello, H. F. Wittmann, R. H. Friend, *Adv. Mater.*, 1997, **9**, 230-232.
- [27] (a) D. V. O'Connor, D. Phillips, *Time-correlated Single Photon Counting*; Academic Press: New York, 1984; (b) N. Boens, W. R. G. Baeyens, D. D. Keukeleire, K. E. Korkidis, M. Dekker,; New York, 1991; pp 21-45.
- [28] W.W. Qin, N. Basarić, J. Hofkens, M. Ameloot, J. Pouget, J. P. Lefèvre, B. Valeur, E. Gratton, M. andeVen, N. D. Silva, Y. Willaert, K. Engelborghs, A. Sillen, G. Rumbles, D. Phillips, A. J. W. G. Visser, A. V. Hoek, J. R. Lakowicz, H. Malak, I. Gryczynski, A. G. Szabo, D. T. Krajcarski, N. Tamai, A. Miura, *Anal. Chem.*, 2007, **79**, 2137-2149.
- [29] Z. Markova, A. B. Bourlinos, K. Safarova, K. Polakova, J. Tucek, I. Medrik, K. Siskova, J. Petr, M. Krysmann, E. P. Giannelis, R. Zboril, *J. Mater. Chem.*, 2012, **22**, 16219-16223.
- [30] S. Sahu, B. Behera, T. K. Maiti, S. Mohapatra, *Chem. Commun.*, 2012, **48**, 8835-8837.
- [31] Z. Yang, M. H. Xu, Y. Liu, F. J. He, F. Gao, Y. J. Su, H. Wei and Y. F. Zhang, *Nanoscale*, 2014, **6**, 1890-1895
- [32] X. F. Jia, J. Li, E. K. Wang, *Nanoscale*, 2012, **4**, 5572-5575.
- [33] Z. Lin, W. Xue, H. Chen, J. Lin, *Anal. Chem.*, 2011, **83**, 8245-8251.
- [34] H. Zhu, X. Wang, Y. Li, Z. Wang, F. Yanga and X. Yang, *Chem. Commun.*, 2009, 5118-5120.
- [35] A. Jaiswal, S. S. Ghosh and A. Chattopadhyay, *Chem. Commun.*, 2012, **48**, 407-409.

[36] H. T. Li, Z. H. Kang, Y. Liu, S. T. Lee, *J. Mater. Chem.*, 2012, **22**, 24230-24253.



## Graphical Abstract

## Scheme 1:



Fluorescence image of SMMC-7721 cells excited by ultraviolet light: a-Milk-CDs; b-S-CDs; c-N-CDs;